A HYPERON BEAM IN TARGET-AREA 2

D. Berley
Brookhaven National Laboratory

G. Bingham
National Accelerator Laboratory

and

G. Conforto
University of Chicago

ABSTRACT

Two possibilities for a relatively simple negative hyperon beam to be installed in area 2 are discussed. A survey experiment using a DISC Cerenkov counter is proposed.

INTRODUCTION

Hyperon beams at the 200-GeV accelerator will provide greater hyperon intensities than available at other lower energy accelerators. As a result, a new and powerful technique will be available to study weak decays as well as hyperon-proton scattering. There are many new experimental problems associated with this technique, and in order that the 200-GeV accelerator be fully exploited for hyperon physics within a few years, it is important that preliminary hyperon experiments proceed shortly after the accelerator starts operating.

The special requirements of the hyperon beam pose a problem about its location and its compatibility with more conventional experiments. First, the hyperon beam cannot share the same target as other experiments. A second special character is that the detection equipment is very close to the target. This report is concerned with the resolution of these problems.

The simplest hyperon beam consists of a channel surrounded by heavy shielding and placed in a magnetic field. In Fig. 1, such a beam is illustrated. The length of the shield is 6-10 meters and is sufficient to absorb the hadronic component produced at the target, except that which emerges, magnetically analyzed, from the channel.

The detection apparatus would start at the end of the channel and extend perhaps 30-100 meters further downstream.

A number of proposals have been offered about how to deal with the compatibility of a hyperon beam and other beams. Of these there are two acceptable solutions. One consists of installing a second target box along side the one already planned for target-area 2. This is shown in Fig. 2. The disadvantages of this scheme are that the experimental arrangement is confined to one side of the hyperon beam line and that the apparatus is inaccessible while the other target is in use.

The second proposal would utilize protons from the diffracted proton beam. While the intensity in the diffracted beam is reduced by a substantial factor, the hyperon experiment could operate independently of other experiments.

The choice between these two depends upon the solution to the problem of the large muon flux emerging from the hyperon beam shield. Whether the utilization of the diffracted proton beam is attractive depends upon the hyperon fluxes. The proton intensity available with the second target box is $\sim 10^{13}$ protons per pulse, with the diffracted beam $\sim 10^{10}$ protons per pulse.

MUON SHIELDING

Muon trapping may simplify the problem of disposing of the muons born between the target and the hadron shield. The trapping principle relies on the fact that the direction of the magnetic field reverses upon traversing the current carrying coils when going from the magnet gap to the magnet yoke. The force experienced by a particle reverses as the particle crosses the coil. The magnetic gradients in the coil are such as to focus the particles in a way that, ignoring energy loss, they exercise a periodic motion about the coil, the positive muons oscillating about one side of a coil, the negative muons about the other. Since the muon source is, to a high degree of accuracy, a line source, the oscillations will have an amplitude of the order of the distance between the beam line and the coil.

The trapping dynamics have been calculated and are understood for the 25-GeV hyperon experiment at the AGS. There the muons are concentrated about the coils when they emerge from the hadron shield and the detection apparatus can be designed to cope with a concentrated rather than a diffused muon source.

There are qualitative differences between a low-energy experiment and a high-energy experiment. In the low-energy experiment, the muons lose a significant fraction of their energy upon traversing the shield (7 GeV in 6 meters of iron). The energy loss damps the oscillation amplitude to concentrate the muons. In the high-energy experiment, the damping is smaller and the wave length of oscillation is longer. The trapping which is so effective at lower energy may be less so at high energy. We are,

however, confident that when the muon trapping problem is fully understood, it will simplify the shield required to dispose of the muons.

The traditional way to handle the muons is to construct a shield so thick that the radiation emerging is at a tolerable level. The thickness required is just proportional to the range of the maximum energy muon to be brought to rest. We have computed the integral spectrum of muons from pi decay per meter of decay length with momentum less than p and found[1] the approximate relation,

$$N(p_\mu < p) \simeq \text{const.} \times 10^{-\left(\frac{p}{28\ \text{GeV}}\right)}.$$

With this expression we compute the ratio of shield lengths required with 10^{13} protons on target and 10^{10} protons on target to produce the same radiation level at the end of the shield with the result that shield length (10^{13}): shield length $(10^{10}) = 2.2$. By reducing the intensity by a factor of 1,000, the shield is reduced by about half. We therefore conclude that the diffracted beam with an intensity of 10^{10} protons requires a large expenditure for shielding, about half that needed for a beam with the full proton intensity.

The shielding for the second target box solution may very well be largely the shielding already provided in area 2.

HYPERON FLUXES

Although the hyperon flux from 200-GeV proton interactions is unknown, we can make a guess about what to expect. An approximate flux formula is derived in Appendix I. It roughly agrees with the predictions of Ref. 2.

Using this formula, we find that $2 \times 10^{-8} \Sigma^-$ per interacting proton emerge through a 1 mm diameter hole in the shield. The intensity is proportional to the cube of the hole diameter. Therefore, with 10^{13} interactions we expect $2 \times 10^{5} \Sigma^-$.

The experiments we have thought are interesting in a beam like this all require 1-mm spatial resolution of the Σ^- line of flight. Many of these experiments have been discussed before.[3]

The 1-mm spatial resolution demands that the aperture be kept to 1mm or position defining spark chambers be placed in the beam. In this case, it is the rate at which the spark chambers record which limits the hyperon intensity.

With 10^{10} protons an aperture of 1 cm provides $\sim 10^{5}$ hyperons, the same flux as with 10^{13} protons, but now the hyperon position needs to be defined with a spark chamber, and the proton beam intensity cannot be increased since 10^{5}/pulse is already the maximum rate at which spark chambers can be operated.

If the proton intensity is further reduced and the aperture opened more, the steeply falling production angular distribution begins to decrease the Σ^- signal-to-background noise.

From an unfocused hyperon beam, the hyperon intensity is therefore limited to $\sim 10^5$ hyperons per pulse by spark-chamber counting rates.

In order to utilize the full proton intensity, the construction of a focused hyperon beam which utilizes the small emissivity of the beam is strongly indicated.[3]

We feel that a focused beam is complicated, and the first hyperon experiment might use a simple magnetic channel. We recommend, however, that a place for a target box be reserved for hyperon experiments which utilize the full accelerator intensity.

SURVEY EXPERIMENT USING A DISC COUNTER

Predictions of hyperon production cross sections are at present very uncertain. It therefore seems reasonable to perform first of all a survey experiment, to measure hyperon yields, and possibly polarizations, as a function of momentum and production angle.

This can be done most conveniently with the aid of a DISC Cerenkov counter. Particles emerging from the collimator are momentum analyzed, and a measurement of their β allows identification of the various masses. For a beam momentum of 150 GeV/c a resolution of $\Delta\beta/\beta = 5 \times 10^{-6}$ is needed which can be obtained with a DISC counter of rather conventional design. The DISC counter can have a useful diameter of the order of 10 cm but imposes the limitation that the angular divergence of the beam be 0.1 to 0.2 mrad.[4] The beam emerging from the collimator can be matched to the DISC counter provided (see Appendix II), $2\Phi W \approx 10$ mm-mrad or $3W(\text{mm})/L(\text{m}) \times W(\text{mm}) = 10$ mm-mrad. For a beam momentum of 150 GeV/c a 40 kG magnet with L = 6 meters gives $\theta = 50$ mrad. For this choice of the parameters of the magnet one has W = 4.5 mm. The maximum horizontal angular spread of the beam is then ± 1.1 mrad and in each point of the aperture, the spread is ± 0.37 mrad. The effective target dimension in the horizontal plane is 9 mm and the momentum spread of the beam is $\Delta p/p = 6\%$.

This source is matched to the DISC by two standard NAL beam transport quadrupoles, the first horizontally defocusing, the second horizontally focusing, of focal lengths ~ 4.5 m and 13 m respectively. The total length of the system, including the magnet, is about 15 meters and the emerging beam has a full divergence of 0.22 mrad in the horizontal plane and 0.175 mrad in the vertical plane. The acceptance in the vertical plane, limited by the opening of the quadrupoles, is 10 mrad.

The stated beam divergence and the required resolution impose for the DISC counter a Cerenkov angle of about 30 mrad, which in turn implies a length of the counter of about 4.5 meters.

From the theoretical predictions for secondary particles at 200 GeV[2] and with the further assumptions that

1. the Σ^+/Σ^- ratio is 2/1 at the target
2. the Σ^-/Ξ^- ratio and Ξ^-/Ω^- ratio are both 100.

The number of particles per 10^{10} interacting protons can be estimated.

The results are measured in the following table:

Particle	Intensity at the Target (Particles/Pulse)	Intensity after 20 Meters
π^-	2×10^4	2×10^4
K^-	4×10^2	4×10^2
$\bar{p}$	20	20
Σ^-	2×10^5	8×10^3
Ξ^-	2×10^3	100
Ω^-	20	0.02

These rates pose a problem to the DISC counter which can handle 10^6 to 10^7 particles/second and which has a rejection ratio of about 10^{-6}. The same setup is of course also useful to look for yet undetected negative stable particles (heavier hyperons, quarks).

APPENDIX I. HYPERON FLUXES

The Σ^- hyperon fluxes expected at the 200-GeV accelerator have been computed assuming that the longitudinal and transverse momentum spectra of hyperons is similar and proportional to that of protons from inelastic collisions at 30 GeV. The partial cross section yielding Σ^- hyperons is assumed to be 1% of the inelastic p-nucleus cross section and independent of incident proton energy.

The most thorough measurement of inelastic proton-proton scattering cross sections has been made by Anderson et al.[5] at 30 GeV. Their data are summarized by an empirical formula which is graphed in Fig. 3. The data do not extend to small enough angles to be directly applicable here. For example, for 20-GeV secondary protons the smallest transverse momentum measured in this experiment is 0.29 GeV/c. Nevertheless, the small angle scattering must join smoothly onto the large angle scattering. In the model of Hagedorn-Ranft,[6] the small angle distribution in p_T is approximately gaussian. Dekkers et al.[7] speculate from their forward production data, which has a resolution in transverse momentum of 0.1 GeV/c, that the transverse momentum

distribution is exponential. Both of these conjectures about the forward scattering cross section are illustrated in Fig. 3. We are thereby led to the following approximations for the baryon spectrum in the small transverse momentum regime.

$$\frac{\partial^2 N}{\partial\Omega\,\partial p} = F_H(E_i)\, p^2\, e^{-p_T^2/\langle p_T^2\rangle}_{HR}, \quad \text{(Hagedorn-Ranft)}$$

$$\frac{\partial^2 N}{\partial\Omega\,\partial p} = F_D(E_i)\, p^2\, e^{-p_T/\langle p_T\rangle}_{D}, \quad \text{(Dekkers et al.)}$$

We now constrain the hyperon cross section to be independent of energy and equal to 1% of the total, and we obtain

$$\frac{\partial^2 N}{\partial\Omega\,\partial p} \simeq 3.2\,\frac{p^2}{E_{inc}}\, e^{-p_T^2/\langle p_T^2\rangle}_{HR}, \quad \text{(Hagedorn-Ranft)}$$

$\frac{\partial^2 N}{\partial\Omega\,\partial p}$ = number of hyperons per interacting proton/GeV-sr

p = hyperon momentum, GeV/c

E_{inc} = incident proton energy, GeV/c

p_T = transverse hyperon momentum, GeV/c

$\sqrt{\langle p_T^2\rangle} = 0.3$ GeV/c.

The value of $\langle p_T^2\rangle$ is a guess. The exponential form from Dekkers et al. gives approximately the same result if $\langle p_T\rangle = 0.25$ GeV.

These estimates agree with Walker[2] and give us confidence that there is no large error in the program of Ranft, whose results were used last year.[3]

It may be that the dominant process by which hyperons are made is through the decays of $N^*_{I=0}$ states which are excited by the scattering collision.[7] These resonances must then have a branching of ~2-3% into hyperons to account for the observed K^+ flux.[2] The neutral N^* decays equally into Σ^+ and Σ^- while the charged N^* never decays into Σ^-. In nuclear collisions perhaps 1/2 of the collisions yield an N^{*o} which can decay into a Σ^-. The assumption that about 1% of the collisions produces a Σ^- is consistent with N^* production as the dominant mechanism for hyperon production.

APPENDIX II. CHARACTERISTICS OF THE COLLIMATOR-MAGNET SYSTEM

Figure 4 shows the horizontal cross section of a collimator of length L and horizontal final aperture W placed in a vertical magnetic field of length L.

Assuming a point target, from simple geometrical considerations, one has the horizontal angular acceptance of the collimator as $\pm\theta = \pm W/2L$, the maximum horizontal angular spread of particles emerging from the collimator as $\pm\Phi = \pm 3\theta = \pm 3W/2L$, and the maximum horizontal angular spread at any point of the aperture as $\pm\theta$. The effective target dimension in the horizontal plane is $\pm W$. The maximum momentum spread of particles emerging from the collimator is $\Delta p/p = \pm 4\theta/\Theta = \pm 2W/\Theta L$, where Θ is the bending angle provided.

REFERENCES

[1] The pion spectrum was computed from CKP formula, Lawrence Radiation Laboratory, UCRL-10022, Jan. 1967, p. 167, for 200-GeV protons incident.

[2] T. G. Walker, Secondary-Particle Yields at 200 GeV, National Accelerator Laboratory 1968 Summer Study Report B. 5-68-24, Vol. II, p. 59.

[3] D. Berley et al., Hyperon Beams at a 200-GeV Accelerator, National Accelerator Laboratory 1968 Summer Study Report B. 10-68-37, Vol. II, p. 233; T. Romanowski, Hyperon Beams at the 200-GeV Weston Accelerator and Possible Experiments with these Beams, National Accelerator Laboratory 1968 Summer Study Report C. 1-68-19, Vol. III, p. 17.

[4] O. Danielsson et al., CERN/ECFA 67/16, Vol. I, p. 357.

[5] Anderson et al., Phys. Rev. Letters 19, 198 (1967).

[6] Hagedorn-Ranft, ECFA, Vol. I, p. 69.

[7] Dekkers et al., Phys. Rev. 157, B962 (1965).

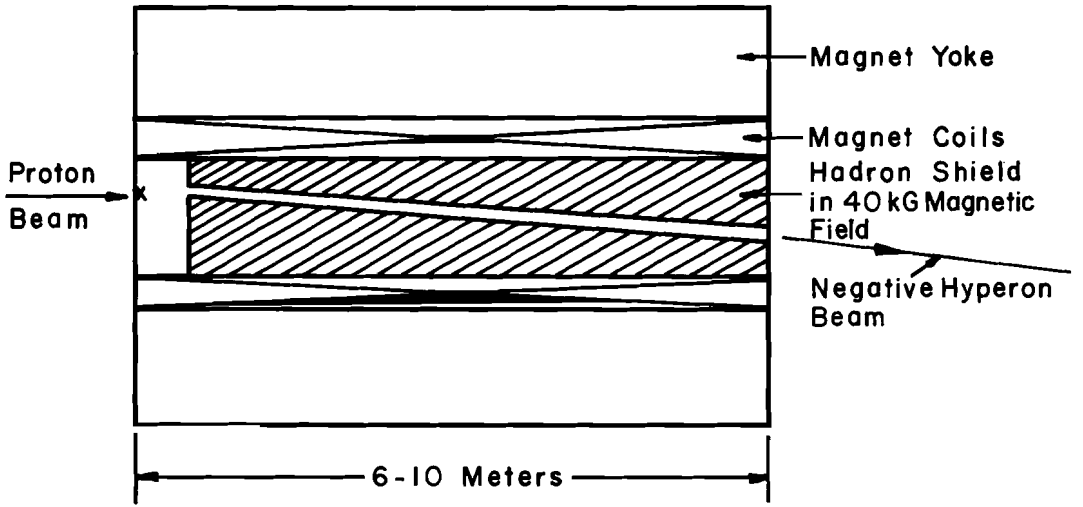

Fig. 1. Target, hadron shield, and magnetic channel for production of high-energy negative hyperon beam.

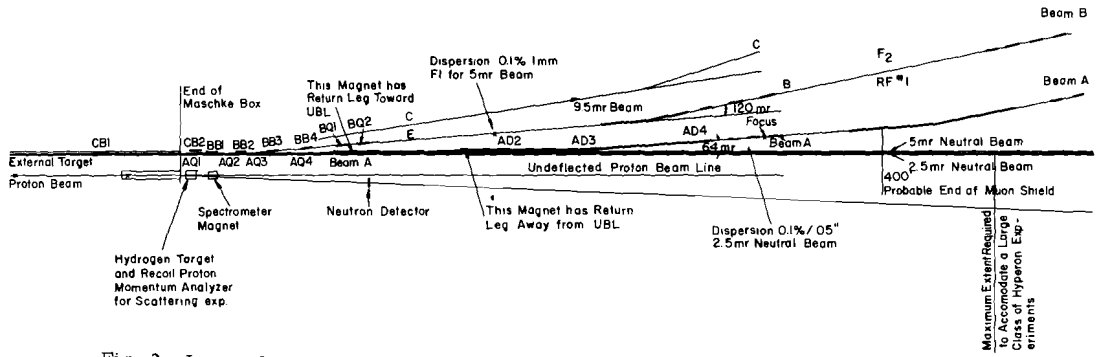

Fig. 2. Layout for hyperon beam (shown with neutron detector) using special branch of incident proton beam.

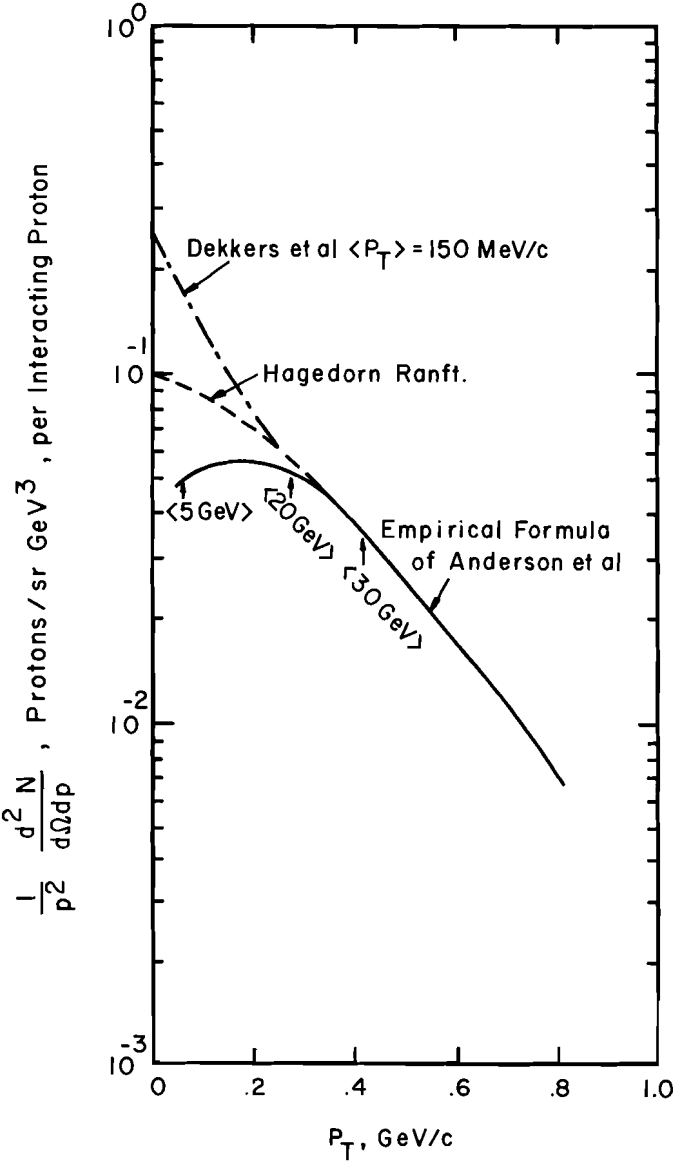

Fig. 3. Transverse momentum spectrum of inelastic proton scattering at 30 GeV/c.

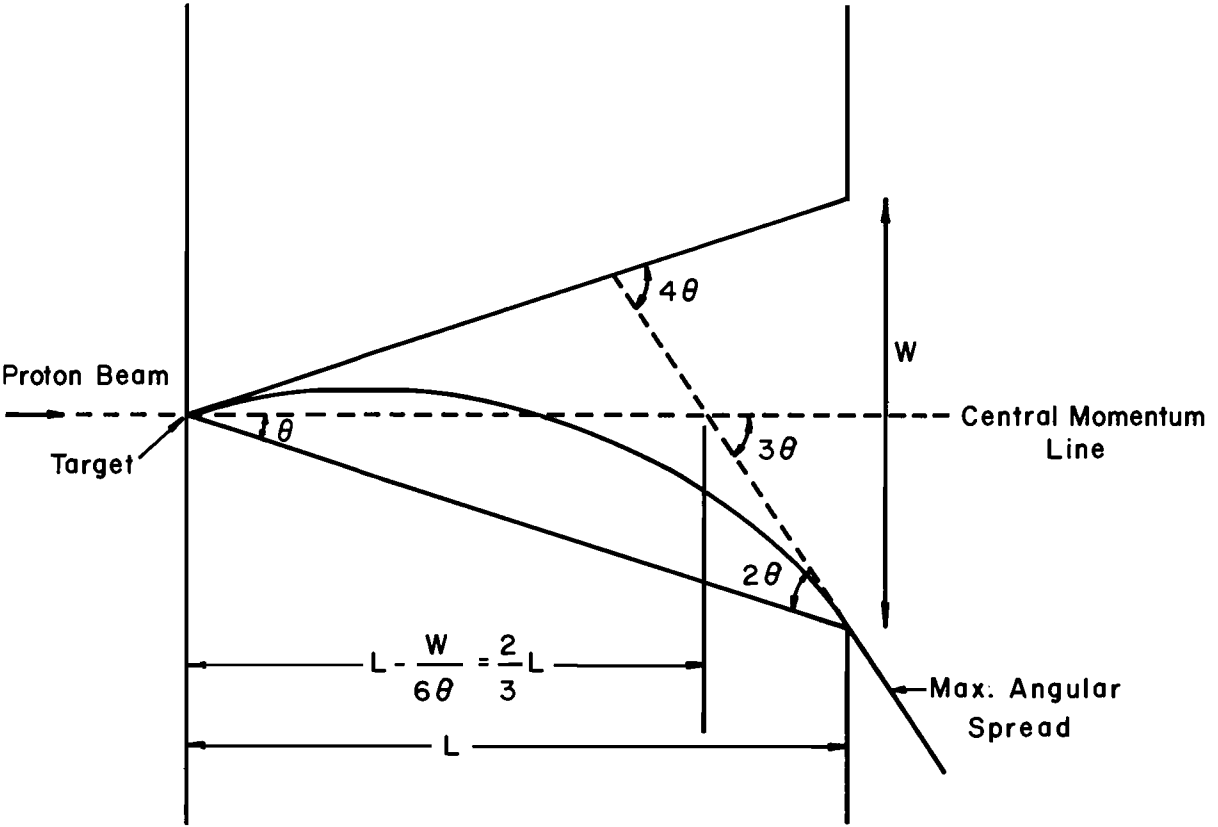

Fig. 4. Horizontal cross section of a collimator of acceptance half-angle θ, in a magnetic field.